X01-Homogenization : implementation and validation

Tutors :

-François ALOUGE

-Sonia FLISS

ENSTA

IP PARIS

Introduction to periodic homogenization

Hugo Negrel

Mars 2022

Contents

1 Introduction

This report is in response to the second practical exercise in the Analysis, Modelisation and Simulation (AMS) Master 2 X01 course. In this case, it concerns the numerical resolution of the cell and homogenisation problem in a domain of dimension 2. Thus, the first part concerns the exact resolution of the diffusion equation for several different periodic tensors A. The second part involves solving the cell problem in order to determine the two correctors. The third part involves solving the homogenised problem with the effective matrix found in the previous part. Finally, this report will conclude by taking a step back from the results found thanks to error estimates when the parameter ϵ tends towards O.

2 Exact solution

Consider the following general problem:

(1)
$$\begin{cases} -\operatorname{div}(A_\epsilon \nabla u_\epsilon) = f & \text{dans} \quad \Omega, \\ u = 0 & \text{sur} \quad \partial\Omega. \end{cases}$$

f is assumed to have regularity $L^2(\Omega)$, $A_\epsilon = A(\frac{x}{\epsilon})$ is a ϵ-periodic tensor satisfying the coercivity and uniform continuity hypothesis. In the same way as in TP1, it is easy to show that the strong formulation is equivalent to the following variational formulation:
$\forall v \in H_0^1(\Omega)$

$$\int_\Omega \vec{\nabla} v \cdot A_\epsilon(x_1, x_2) \cdot \vec{\nabla} u_\epsilon \, \mathrm{d}x = \int_\Omega f v \, \mathrm{d}x,$$

which has a unique solution according to the Lax-Milgram theorem. The continuity of the second and first member is obvious. The same applies to the coercivity with the semi-norm of $H_0^1(\Omega)$. We therefore reuse the code from TP1, omitting the mass matrix in the EF matrix. The code will be tested for different A scattering matrices. The test case will be for $A = Id$. We impose the solution $u(x_1, x_2) = \sin(\pi x_1) \sin(\pi x_2)$ and then deduce the corresponding source function. $f(x_1, x_2) = (1 + 2\pi^2) sin(\pi x_1) \sin(\pi x_2)$ is the source function in this simple case.

The source function differs depending on the case studied.

- A = Id : $f = (1 + 2\pi^2) \sin(\pi x_1) \sin(\pi x_2)$,

- case (i) : $f = 3\pi^2 \sin(\pi x_1) \sin(\pi x_2)$,

- case (ii) : $f = -\pi^2(2\cos(2\pi x_1)\cos(\pi x_1)\sin(\pi x_2) - (2 + \sin(2\pi x_1))\sin(\pi x_1)\sin(\pi x_2) - 4\sin(\pi x_1)\sin(\pi x_2))$,

- case (iii) : $f = -\pi^2(2\cos(2\pi x_1)\cos(\pi x_1)\sin(\pi x_2) - (2 + \sin(2\pi x_1))\sin(\pi x_1)\sin(\pi x_2) - (4 + \sin(2\pi x_1))\sin(\pi x_1)\sin(\pi x_2))$,

- case (iv) : $f = -\pi^2(2\cos(2\pi x_1)(4 + \sin(2\pi x_2))\cos(\pi x_1)\sin(\pi x_2) + 2(2 + \sin(2\pi x_1))\cos(2\pi x_2)\sin(\pi x_2)\cos(\pi x_2) - 2(2 + \sin(2\pi x_1))(4 + \sin(2\pi x_2))\sin(\pi x_1)\sin(\pi x_2))$.
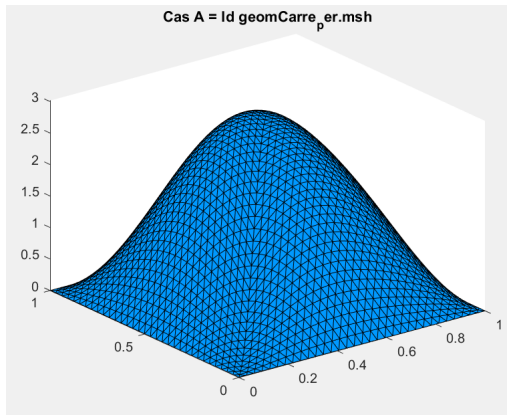
Depending on the tensor considered, we obtain

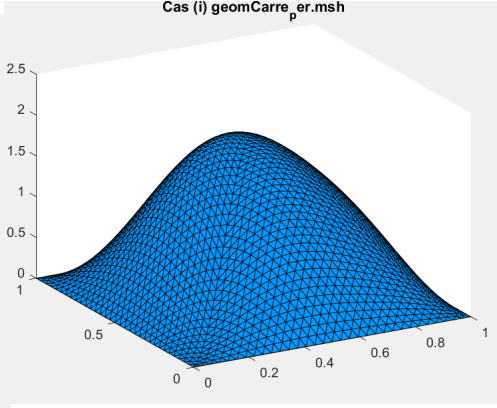Figure 1: Exact solution for A = Id.

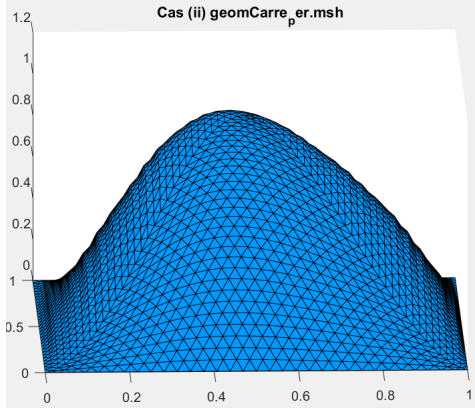Figure 2: Exact solution for the case (i).
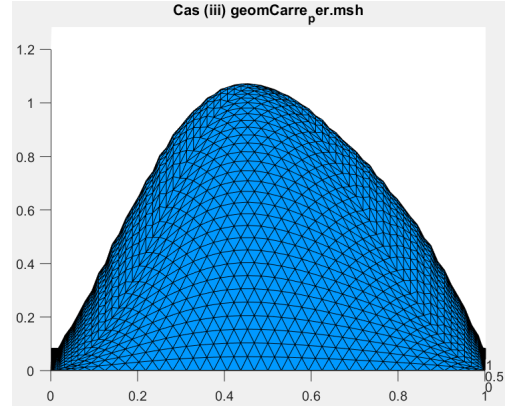

Figure 3: Exact solution for the case (ii).

Figure 4: Exact solution for the case (iii).

What is interesting is the appearance of small oscillations in the figures, particularly along the slope when the A tensor is no longer homogeneous. This is compatible with what is expected, and justifies a priori a power decomposition of ϵ as presented in the course.
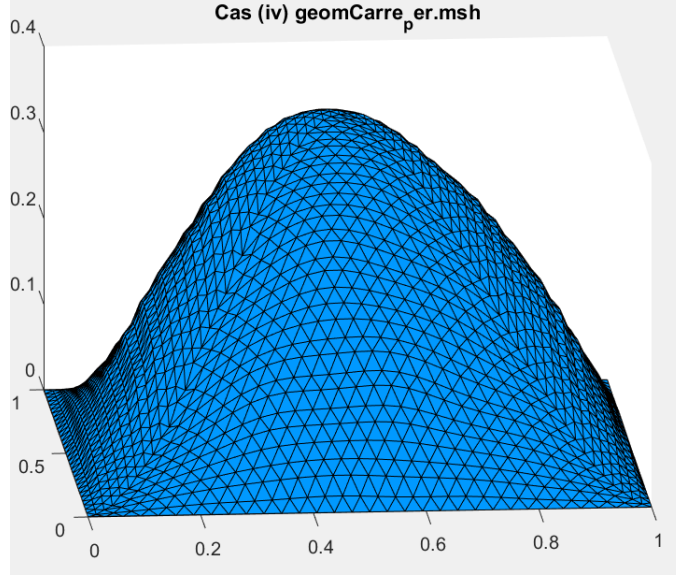
4

Figure 5: Exact solution for the case (iv).

3 Solution of the homogenised problem

3.1 The cell problems

The space $V = \in H^1_{mbox\#}(Y)/\int_Y \psi(y)dy = 0\}$ is given the norm $||cdot||_{H^1(Y)}$. V is a Hilbert space as a closed subspace of a Hilbert space, since the application $:\psi \longmapsto \int_Y \psi dy$ is continuous in $H^1(Y)$. Let

$$a : (u,v) \longmapsto a(u,v) = \int_Y (A(y)\nabla_y w_i(y), \nabla_y \phi(y))dy$$

, $\forall(u,v) \in V$. By the coercivity property of A, we have directly $a(u,u) \geq c||u||_{H^1_0(Y)}$. This form is also bilinear and continuous, given the uniform continuity property of A. The form $l : u \longmapsto l(u) = -\int_Y (A(y)e_i, \nabla_y u(y)dy$ is linear and continuous in V. According to the Lax-Milgram theorem, there is a unique solution in V to the variational problem.

To facilitate the numerical discretisation of the zero mean condition for the test functions, we return to the space $H^1_\#(Y)$ (with the $||\cdot||_{H^1(\Omega)}$ norm) and change a. We now take: $a' : (u,v) \longmapsto \int_Y (A(y)\nabla_y w^\eta_i(y), \nabla_y \phi(y)) + \eta \int_Y w^\eta_i(y)\phi(y)dy$. It is equally straightforward to see that, η being positive, we have $a'(u,u) \geq min(1,\eta)||u||_{H^1(\Omega)}$. a' remains bilinear and continuous. Once again, according to the Lax-Milgram theorem, there is a unique solution to the variational formulation: Find $w^\eta_i \in V$ such that $\forall \phi \in V$

$$\int_Y (A(y)\nabla_y w^\eta_i(y), \nabla_y \phi(y)) + \int_Y w^\eta_i(y)\phi(y)dy = -\int_Y (A(y)e_i, \nabla_y u(y)dy.$$

5

Naturally, the coercivity constant decreases with η, which suggests that the data control constant will become worse and worse, i.e. larger and larger:

$$||w_i^\eta||_{H^1(\Omega)} \leq C'||f||_{L^2(\Omega)}$$

where we have $C' \propto 1/c$. The consequence of this is that the matrix becomes 'less and less invertible', i.e. the inversion of the matrix risks being less stable and more subject to rounding errors (conditioning increases).

Note that $\int_Y w_i^\eta dy = 0$ and therefore that $\int_Y (w_i^\eta - w_i) dy = 0$. This is straightforward if we take $\phi(y) = $ cte. Subtract (3) by (2) and taking $\phi = w_i^\eta - w_i \in V$), we then have

$$\int_Y (A(y)\nabla(w_i^\eta - w_i), \nabla(w_i^\eta - w_i))\mathrm{dy} + \eta \int_Y (w_i^\eta - w_i)^2\mathrm{dy} = \eta \int_Y w_i(w_i - w_i^\eta)\mathrm{dy}.$$

By placing ourselves in the space V, we can use the Poincaré-Friedrichs inequality, as well as using the fact that A is a coercive and continuous tensor, we can easily show that the norm $|\phi|^2 = \int_Y (A(y)\nabla\phi(y), \nabla\phi(y)\mathrm{dy}$ is equivalent to the norm $||\cdot||_{H^1(\Omega)}$. Since $\eta \geq 0$, we naturally have

$$|w_i - w_i^\eta|^2 \leq \int_Y (A(y)\nabla(w_i^\eta - w_i), \nabla(w_i^\eta - w_i))\mathrm{dy} + \eta \int_Y (w_i^\eta - w_i)^2\mathrm{dy}$$

. In addition,

$$\eta|\int_Y w_i(w_i - w_i^\eta)\mathrm{dy}| \leq \eta||w_i||_{L^2(\Omega)}||w_i - w_i^2||_{L^2(\Omega)} \leq \eta||w_i||_{L^2(\Omega)}||w_i - w_i^2||_{H^1(\Omega)},$$

and by equivalence of the norms $|\cdot|$ and $|\cdot||_{H^1(\Omega)}$, we have by minimization :

$$C'||w_i - w_i^\eta||^2_{H^1(\Omega)} \leq |w_i - w_i^\eta|^2 \leq ||w_i||_{L^2(\Omega)}\eta||w_i - w_i^\eta||_{H^1(\Omega)}.$$

Finally, $\exists C \geq 0$, independent of η,

$$||w_i - w_i^\eta||_{H^1(\Omega)} \leq C\eta,$$

which was the result to be demonstrated.

3.2   Discretization of cell problems

The variational formulation is simple to solve, just use the code from TP1 in the periodic case by simply adding the η parameter. As far as the second member is concerned, we can see that we can find the stiffness matrix if we note that $e_i = \nabla x_i$. By storing the abscissa and ordinate values of each of the vertices in lists, it is then easy to calculate the second member in the case $x_1 = x$ and $x_2 = y$. We can therefore calculate $\mathbf{L}$ exactly:

$$\mathbf{L} = -X^T\mathbf{KK} = -\mathbf{KK}X,$$

by symmetry of $\mathbf{KK}$ and where X is the list of abscissas in the case $i = 1$ and the list of ordinates for $i = 2$ of the Lagrange points. As far as the pseudo-elimination method is concerned, we do exactly the same as in TP1, i.e. we use the appropriate transition matrix.

3.3   First validation

We know that when $A = Id$ and in case (i), the correctors will necessarily be zero. This can be demonstrated with the variational formulation, or intuited by noticing Q1) that there is no oscillation on the exact solution, which suggests that $u_1 = 0$ from the ansatz: $u_{epsilon}(x, \frac{x}{\epsilon}) = u_0(x) + \epsilon u_1(x, \frac{x}{\epsilon}) + \epsilon^2 u_2 + ...$ I chose the value of $\eta = 0.01$, a value that is neither too large to give a good approximation nor too small to avoid errors in numerical calculations that are too coarse when the finite element matrix is inverted.
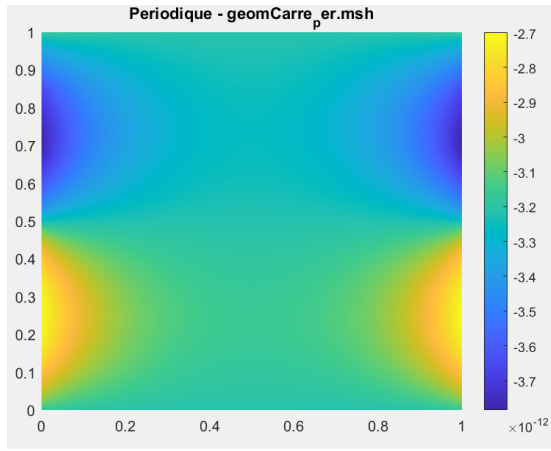
The numerical simulation confirms this:

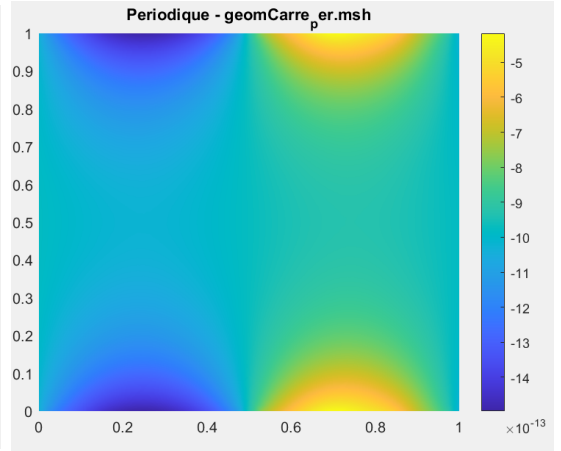Figure 6: Corrector w_{x_1} for $\eta = 0.01$.

Figure 7: Corrector w_{x_2} for $\eta = 0.01$.

3.4   Homogenised tensor calculation and second validation

The calculation of the coefficients of the tensor A_{eff} in the basis (e_x, e_y) is very simple, it is sufficient to use once again that $\nabla y_i = e_i$ and thus to invoke the stiffness tensor in the finite element calculation. The calculation is shown at the end of the code solving the cell problem. After calculating the two correctors using the 'Principal-periodiq-cell' routine, we obtain the effective diffusion matrix A_{eff}.

It then becomes very simple to solve the homogenised problem, and we find ourselves in the same situation as in TP1 with the Dirichlet conditions.

4   Comparison of the exact solution and the solution of the homogenised problem

We observe that the homogenised solution is smooth compared to the solution of the complete problem: the wavelets appearing in Q1 have disappeared.
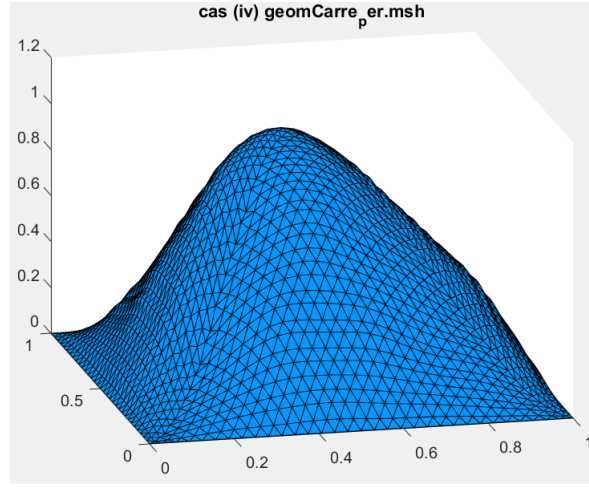
Figure 8: Solution of the homogenised problem in case (iv)

.

For case (iv), we obtain figures 9 and 10.

With regard to the influence of ϵ, we can see that the amplitude of the $\approx \epsilon$ frequency oscillations decreases as ϵ approaches 0. This is due to the very particular convergence which is the double-scale convergence, erasing the ϵ frequency oscillations.
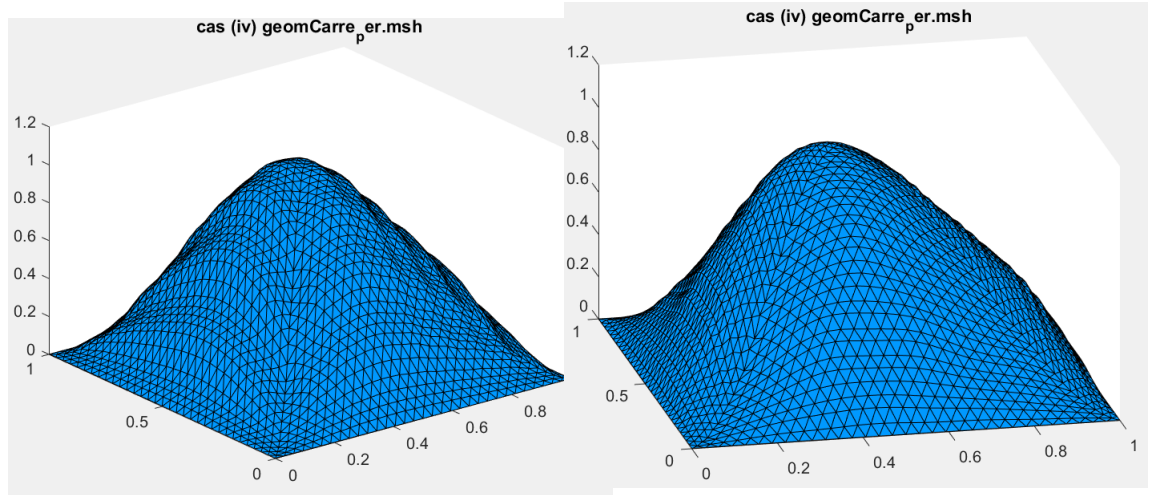

Figure 9: Solution for the case (iv) with $\epsilon = 0.1$.

Figure 10: Solution for the case (iv) with $\epsilon = 0.01$.

However, in order to obtain a more quantitative result, we would like to look

at the evolution of the norms $L(Y)^2$ and $H^1(Y)$. However, it is ϵ that will be varied and not the mesh pitch. The errors (see Figures 11 and 12) increase very quickly, as can be seen on the error curves, when the pitch becomes of the same order of magnitude as ϵ. I decided to vary ϵ from 0.5 to 10^{-4} with a step size of 0.1. I also used a mesh size of about $1/64$, so as not to take too long to calculate. I will present the curves in case (iv) because it is similar to the most general case proposed: A depending on x and y. The solution u_0 **is not** equal to $u(x_1, x_2) = \sin(\pi x_1)\sin(\pi x_2)$ when $epsilon \neq 1$. As a result, it's not surprising to see a rotational asymmetry appear even if u doesn't show any. To calculate the error, we need to compare u_0 and $u_{0,h}$, both calculated numerically. We must therefore first calculate u_0 by solving the homogenised problem, and then compare it with $u_{0,h}$ as we did in TP1.
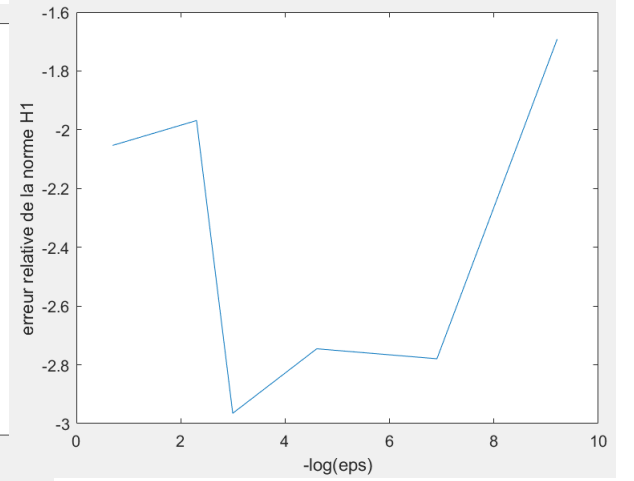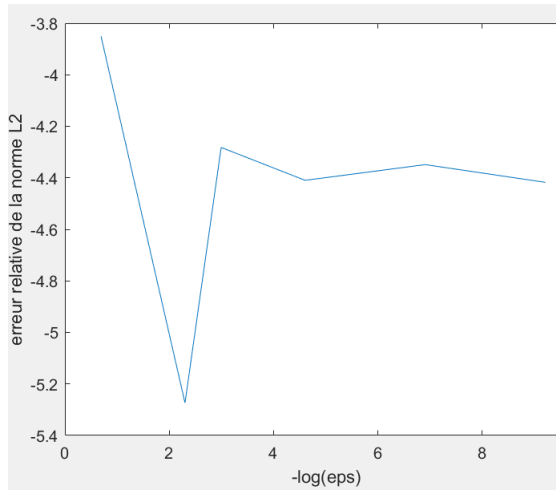

Figure 11: $||u_0 - u_{0,h}||_{L^2(\Omega)}$ as function of ϵ.   Figure 12: $||u_0 - u_{0,h}||_{H^1(\Omega)}$ as function of ϵ.

If we want to improve the estimate in H^1, the course teaches us that this is possible. Under certain assumptions about the regularity of the solutions, which I will not go into in detail, we can show that $||u_\epsilon - (u_0 + \epsilon(\partial_{x_1}u_0(x)w_1(x/\epsilon) + \partial_{x_2}u_0(x)w_2(x/\epsilon))||_{H^1(\Omega)} = \mathcal{O}(\epsilon)$. We have shown this rigorously in $\mathbb{R}^d$, but we can apply it here without any problems to this bounded domain by neglecting boundary layer effects. The challenge is to calculate the partial derivatives of u_0 on each vertex of the triangulation. To do this, the idea is to return to the reference triangle using a canonical affine transformation, the same as that used to calculate the stiffness and mass matrices. As in TP1, we introduce the affine transformation

$$F \ : \ \begin{matrix} \hat{M} & \to & M \\ \hat{x} & \mapsto & F(\hat{x}) = A\hat{x} + B \end{matrix}$$

On the reference triangle, the axes $e_{\hat{x}_1}$ and $e_{\hat{x}_2}$ are well defined and will be the same on each of the Ω finite elements, which makes the task much easier. By

9

composition, we have

$$\partial_{x_1} u_0 = \partial_{\hat{x}_1} u_0 \partial_{x_1} \hat{x}_1 + \partial_{\hat{x}_2} u_0 \partial_{x_1} \hat{x}_2.$$

We immediately have $\partial_x \hat{x} = A^{-1}$, and we can deduce from the previous calculation the more general formula

$$\partial_x u_0 = (A^{-1})^T \partial_{\hat{x}} u_0.$$

Let's now concentrate on the term $\partial_{\hat{x}_j} u_0$, $j \in \{1,2\}$. We obviously have the decomposition $u_0(\hat{x}) = \hat{\lambda}_i(\hat{x}) u_0(x_i)$, with $x_i \in \hat{A}, \hat{B}, \hat{C}$. Naturally, $\partial_{\hat{x}_j} u_0(\hat{x}) = u_0(\hat{x_i}) \partial_{x_j} \hat{\lambda}_i(\hat{x})$. In the case $j = 1$, $\partial_{\hat{x}_1} u_0 = -u_0(\hat{A}) + u_0(\hat{B})$ and for $j = 2$, $\partial_{\hat{x}_2} u_0 = -u_0(\hat{A}) + u_0(\hat{C})$ given the local basis functions $\hat{\lambda}_1(\hat{x}, \hat{y}) = 1 - \hat{x}_1 - \hat{x}_2$, $la\hat{m}bda_2(\hat{x}_1, \hat{x}_2) = \hat{x}_1$ and $la\hat{m}bda_3(\hat{x}_1, \hat{x}_2) = \hat{x}_2$. Note that the derivatives do not depend on (x_1, x_2) and so we have the same values of $\partial_{\hat{x}_j} u_0(\hat{x})$ throughout the triangle.
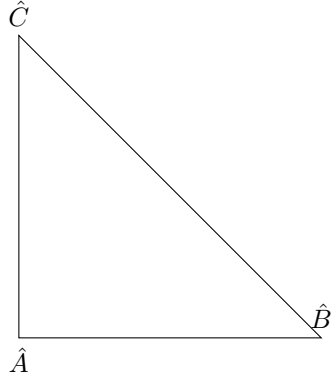
Above is a reference triangle. The vertex $\hat{A}$ has coordinate (0,0), the vertex $\hat{B}$ has coordinate (1,0) and the vertex $\hat{C}$ has coordinate (0,1).

To convince ourselves that the method is not absurd, Figure 13 shows the gradient of u_0, which is compatible with the idea of the gradient we have in Figure 8.

Finally, I obtained this error curve for the H^1 norm (figure 15), which shows an improvement in the approximation of the u_ϵ solution as a function of $H^1(\Omega)$. The slowdown observed for small ϵ can be explained once again by the limits of the result when the discretisation becomes visible for the period of the tensor. However, we do observe a slope of -1 at the beginning of the curve, which is as expected.

5   Conclusion

In conclusion, ϵ must be well controlled according to the mesh size used. The theoretical results between u_0 and u_ϵ do not take into account the discretisation
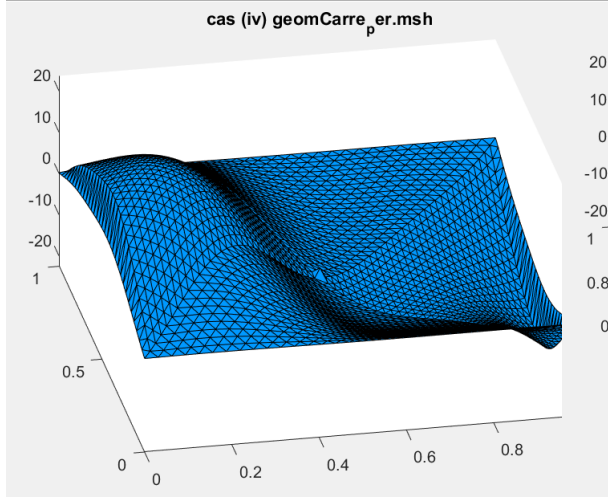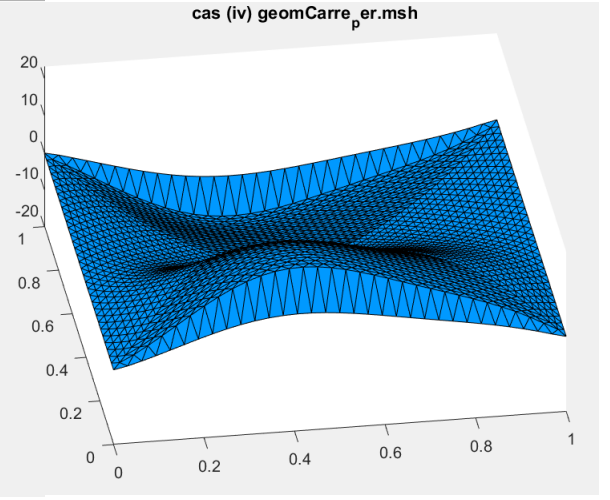
Figure 13: Gradient of u_0 along e_{x_1}.   Figure 14: Gradient of u_0 along e_{x_2}.
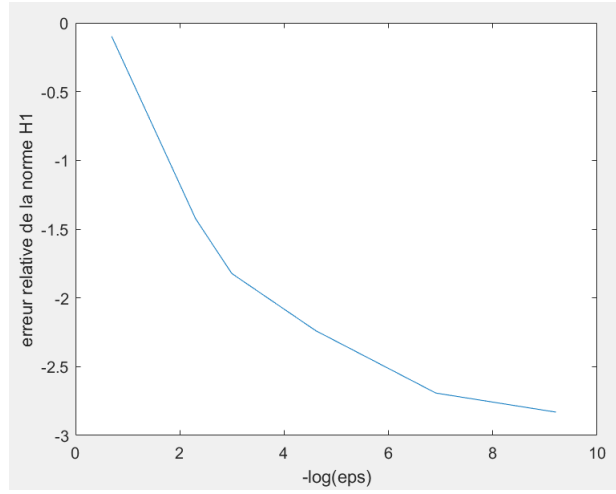

Figure 15: $||u_\epsilon - u||_{H^1(\Omega)}$ as a function of ϵ.

of the vector spaces involved, which must be taken into account when interpreting the convergence results. We cannot expect a near-perfect slope as in TP1. The difficulty therefore lies in choosing ϵ small enough to give a good approximation, but not so small as to be of the same order of magnitude as the mesh pitch.

Several enriching methods have been used here: the calculation of the effective matrix using correctors, which worked very well, or taking account of space constraints by using a η parameter. An interesting test could have been a non-

11

diagonal and non-homogeneous tensor A, in order to treat the most general case possible. However, if the tensor is symmetrical, given that it is positive over the whole domain, it would still have been possible to return to the diagonal case according to spectral theory.

As far as the H^1 approximation is concerned, the theory has been established as well as the associated implementation. There is indeed an improvement in the approximation of the solution in the sense of the H^1 norm.

To sum up, the solution can be calculated as follows:

- A parameter ϵ and η is set according to the mesh size chosen beforehand.

- The two correctors associated with the problem are calculated and the effective matrix is deduced.

- Solve the homogenised problem.

- Solve the diffusion problem as described at the beginning of the tutorial.

- Calculate the partial derivatives of u_0 in each of the triangles.

- Compare the results in terms of the norm L^2 and H^1 using the stiffness and mass matrices.